Packed Bed Combustion of Wood

Elisabeth Girgis[1] and William Hallett[2]
Depts. of [1]Chemical Engineering and [2]Mechanical Engineering
University of Ottawa, Ottawa, Ontario K1N 6N5

Packed bed combustion is widely used for wood waste and other biomass conversion in the pulp and paper industry and in small-scale heating systems as well as for trash incineration. Biomass fuels generally have a very high proportion of volatiles (typically 80- 85% for wood); thus pyrolysis is a very important part of the combustion process. This paper extends earlier work on packed bed combustion [1, 2] to include pyrolysis. Experiments are performed in packed bed combustion of wood and the results simulated by adding a simple pyrolysis model to an existing numerical model for packed bed combustion.

Experiments

The system dealt with here is an overfeed packed bed of fuel particles resting on a grate, through which air streams vertically upwards (Fig. 1). Fresh fuel is fed to the surface to keep the level constant; devolatilization takes place in the top layers of the bed, and the volatiles burn above the bed with secondary air. (Only if the bed is less than two particles thick will oxygen from the primary air be available to burn volatiles within the bed.) Temperatures at various points in the bed are measured by type B thermocouples, and local gas compositions are measured by a water-cooled sampling probe connected to a gas chromatograph. At the conclusion of a test the bed is quenched with nitrogen and cut into slices for subsequent solid sampling and analysis. The reactor diameter was 23 cm and the bed height was maintained at 22 cm for these tests. More details are given in [2].

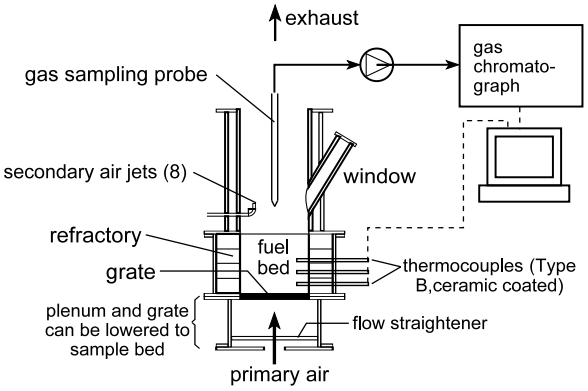

Fig. 1: Cross-section of experimental combustor and instrumentation

A substantial part of the volatiles from wood is a range of heavier species known collectively as tar, and it is desirable to be able to measure its concentration locally in the bed. Sampling using conventional techniques would require a probe heated to 300-400°C by steam jacketing to avoid condensing tar in the probe. A novel probe was therefore designed (Fig. 2), which condenses and collects tar *in situ* in a water-cooled porous metal filter element, allowing determination of the tar mass through weighing. The filter elements were held in a tapered brass collet similar to a lathe collet, which was closed and sealed around the filter by pressure from a threaded cap, all parts being machined to a

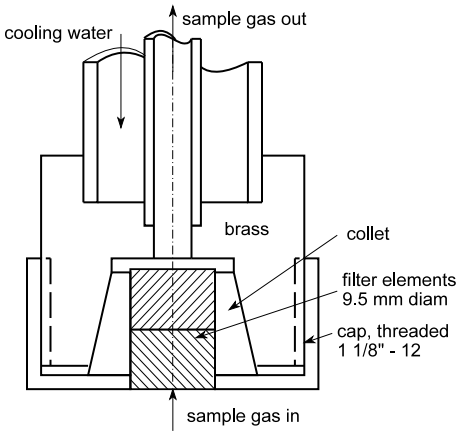

Fig. 2: Cross-section of tip of tar sampling probe.

close fit to avoid gas leakage past the filter. The tar is collected from a metered flow of gas drawn through the probe for a measured time interval, so that the tar can be directly related to other species concentrations in the bed. Like the gas sampling probe, the tar probe is inserted vertically downwards into the desired sampling location in the bed. The probe is backflushed with nitrogen before sampling begins and withdrawn from the bed as quickly as possible after sampling ends so as to avoid errors due to collection of extraneous tar.

The fuel was 1 x 2 spruce lumber cut into parallelepipeds (Fig. 3), this shape being chosen to allow easy calculation of particle equivalent diameter and sphericity while assuring random packing.

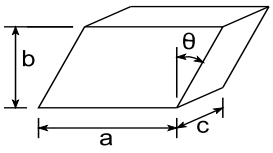

Fig. 3: Fuel particle. a = 3.5 cm, b = c = 1.8 cm, θ = 20°.

Table 1: Experimental Conditions

Fuel volatiles (ASTM, dry basis)	84%
Fuel moisture	6%
Ash (dry basis)	0.3%
Particle size (vol. equiv. diameter)	2.8 cm
Particle sphericity	0.76
Fuel density (kg/m^3)	499
Bed void fraction	0.47
Bed height (cm)	22
Primary air mass flux (kg/m^{2}hr)	109

2. Numerical Model

A numerical model for this process was devised by adding a simple devolatilization reaction to an existing model for packed bed combustion of char. This model, described in detail in [1, 2], includes all relevant processes for char: gas-phase and solid surface reactions, fuel particle consumption and motion, ash layer buildup, heat conduction in the solid phase, heat conduction and diffusion in the gas phase, heat and mass transfer between the particulate and gas phases, properties variations, the effects of ash particles in the voids between fuel particles on heat and mass transfer, and the effects of thermal boundary conditions such as the grate and the freeboard space above the bed. It can also account for non-spherical fuel and ash particles. The governing equations are solved by finite volume techniques to give the details of gas and solid composition and temperature as functions of position and time.

The pyrolysis of large pieces of fuel such as are commonly fired in packed beds is fairly complex. The pyrolysis reaction itself is generally considered to be multi-step, resulting in gases, tar vapours and char as the products [3, 4], although for calculations a single step is often assumed [5]; moreover, with wood fuel each of the three main components (cellulose, hemicellulose, and lignin) may pyrolyze differently [3, 4]. In addition to the chemical reactions, the processes of heat conduction into the solid, gas flow out of the solid, and drying are acknowledged to be important, particularly for large particles. However, as a first step in adding fuel pyrolysis to the existing model, the simplest possible pyrolysis model will be used: a one-step first order chemical reaction, with fuel particles assumed uniform in temperature and composition. Further refinements will follow as the model is developed. The fuel is therefore assumed to pyrolyze with a char yield of ζ_C:

$$1 \text{ kg fuel} \rightarrow \zeta_C \text{ kg char} + (1 - \zeta_C) \text{ kg gas}$$

and the rate is given as

$$\frac{dW}{dt} = -AW\exp(-E/RT) \qquad (1)$$

where W (= "wood") is the mass fraction of original fuel unconverted. The pyrolysis products are assumed to consist of fixed proportions χ_{CO2}, χ_{CO}, and χ_T of CO_2, CO and tar respectively. Since the fuel used in the experiments had a very low moisture content, fuel moisture and the drying process are neglected. As mentioned earlier, unless the bed is less than two particles thick, combustion of pyrolysis products occurs entirely above within the bed, and it is therefore not included in this model.

Pyrolysis must then be accounted for in the conservation equations for the gas and solid phases in the bed. The overall rate of production of pyrolysis products per unit bed volume is

$$r_P = -(1-\epsilon)(1-\zeta_C)\rho_C \frac{dW}{dt} \quad (kg\ gas/m^3\ bed) \tag{2}$$

so that the equation for overall gas phase mass conservation is

$$\frac{\partial}{\partial t}(\epsilon\rho_G) + \frac{\partial}{\partial x}(\rho_G v_G) = Ga_{BC} + r_P \tag{3}$$

where G is the rate of char consumption by oxidation and CO_2 reduction, and a_{BC} is the specific surface area of fuel particles. The rate of production of each individual product is

$$r_{CO2} = \chi_{CO2} r_P; \qquad r_{CO} = \chi_{CO} r_P; \qquad r_T = \chi_T r_P \tag{4}$$

so that the transport equation for tar is

$$\frac{\partial}{\partial t}(\epsilon\rho_G Y_T) + \frac{\partial}{\partial x}(\rho_G v_G Y_T) = \frac{\partial}{\partial x}(\rho_G D_{T\,eff}\frac{\partial Y_T}{\partial x}) + r_T \tag{5}$$

where $D_{T\,eff}$ is the effective diffusivity of tar in the gas phase, determined as in [1]. The r_{CO2} and r_{CO} terms are added to the existing transport equations for CO_2 and CO given in [1].

For the solid phase (fuel and ash together), the overall continuity equation is

$$\frac{\partial}{\partial t}[(1-\epsilon)\rho_S] + \frac{\partial}{\partial x}(\rho_S v_S) = -Ga_{BC} - r_P \tag{6}$$

where v_S is the superficial velocity of the solid phase in bulk. For the fuel particles alone, mass conservation gives

$$\frac{\partial}{\partial t}[(1-\epsilon)\rho_F X_F] + \frac{\partial}{\partial x}(\rho_F v_F) = -Ga_{BC}(1+\alpha) - r_P \tag{7}$$

A third solids conservation equation can be used to keep track of the extent of pyrolysis. This is done through the mass fraction Y_W of unpyrolyzed fuel:

$$\frac{\partial}{\partial t}[(1-\epsilon)\rho_F X_F Y_W] + \frac{\partial}{\partial x}(\rho_F v_F Y_W) = -\frac{r_P}{1-\zeta_C} \tag{8}$$

This can be related to the conversion W as follows: the amount unpyrolyzed is W kg/kg of initial fuel, while the mass of char produced so far is (1 - W) ζ_C, giving the mass fraction Y_W as

$$Y_W = \frac{W}{W + (1-W)\zeta_C} \quad or \quad W = \frac{Y_W\zeta_C}{1 - Y_W(1-\zeta_C)} \tag{9}$$

The fuel particles are assumed not to change size during pyrolysis, so that the char density is $\rho_C = \zeta_C \rho_{F0}$, where ρ_{F0} is the initial fuel density, and the fuel particle density at any time is

$$\rho_F = [Y_W/\rho_{F0} + Y_C/\rho_C]^{-1} = \rho_{F0} [W + (1 - W) \zeta_C] \qquad (10)$$

Char combustion is assumed to follow the shrinking particle model as in [1, 2]. At the particle surface, the net flux of a given species from the surface is given by the sum of convection and diffusion:

$$G_i = (G + G_P) Y_{iR} + k_{Yi}(Y_{iR} - Y_i) \quad (kg/m^2 s) \qquad (11)$$

where $G_P = r_P / a_{BC}$ is the flux of pyrolysis gas, so that the first bracketed term is the total mass flux leaving the surface, and k_{Yi} is the mass transfer coefficient [1]. This equation is combined with reaction rates at the surface to solve for the surface concentration of O_2 and other gases. Note that no explicit decision has to be taken as to whether or not char can react while devolatilization is going on: this is decided by the O_2 concentration at the surface calculated from eq. (11).

Properties are required for wood, char and tar. Correlations for specific heat were taken from [7] for wood and from [8] for char, while thermal conductivities were taken from [6] for wood and [8] for char. A useful compilation of wood and char properties was recently given by Gupta *et al.* [9]. The tar was assumed to have the properties of levoglucosan, a common high molecular weight product of cellulose pyrolysis, and properties - vapour specific heat, diffusivity, and conductivity, and critical state - were estimated using standard correlations [10]. Ash properties were taken from measurements from earlier wood combustion tests [11], which gave a mean particle diameter of 1 mm, a density of 1030 kg/m^3, a sphericity of 0.60, and a void fraction for the ash phase of 0.45.

Results

Figs. 4 - 7 present experimental data from one particular test and compare them to model predictions. At this point, no effort has been made to rigorously fit rate constants to the data. The rates of carbon oxidation and CO_2 reduction are as in [2], while the parameters of the pyrolysis reaction were taken as $A = 0.05\ s^{-1}$, $E = 10\ 000$ J/mol. This is a much lower activation energy than usually given for wood or cellulose [3-5, 7], and reflects the fact that intra-particle heat conduction is expected to play a major role in determining the pyrolysis rate for the fairly large fuel particles used here. An equal split between the three pyrolysis products ($\chi_{CO2} = \chi_{CO} = \chi_T$) gave reasonable product concentrations. The enthalpy of pyrolysis was set to 200 kJ/kg wood (endothermic).

Gas concentrations (Fig. 4) show the typical pattern of packed bed combustion: a thin char oxidation zone at the bottom of the bed, within which all O_2 is consumed, followed by a CO_2 reduction zone in which CO is generated at the expense of CO_2. Fresh fuel fed on to the top of the bed begins to devolatilize and then moves downwards in the bed as the char beneath it is consumed. The pyrolysis process is most clearly reflected in the steep rise in tar, but it also leads to both CO_2 and CO increasing as well as the top of the bed is approached. The predicted concentrations of gaseous species agree well with the data and could probably be made to agree better with proper fitting of rate parameters. The biggest source of disagreement is stochastic variations in conditions at the probe tip: owing to the random packing and settling of particles, the local geometry of the bed is continually varying on a scale of about half a particle diameter, leading to considerable scatter in

quantities measured at different times at a given point.

The tar and CH_4 data suggest that pyrolysis is spread out over a larger region of the bed than predicted, and this is consistent with the neglect of heat conduction inside the particle in the model. Reducing the rate of pyrolysis produced better agreement, but at the expense of having pyrolysis continue to an unreasonably low level in the bed. However, this does not explain the roughly constant level of tar observed: one would still expect the tar level to rise towards the top of the bed as more tar is added to the flow. This behaviour may indicate the action of gas phase secondary cracking reactions decomposing the tar into gaseous products after it is produced. Tar data for other experimental runs showed similar trends. The peculiar dip in tar concentration at a height of about 15 cm was observed in most runs, and is further suggestive of secondary reaction.

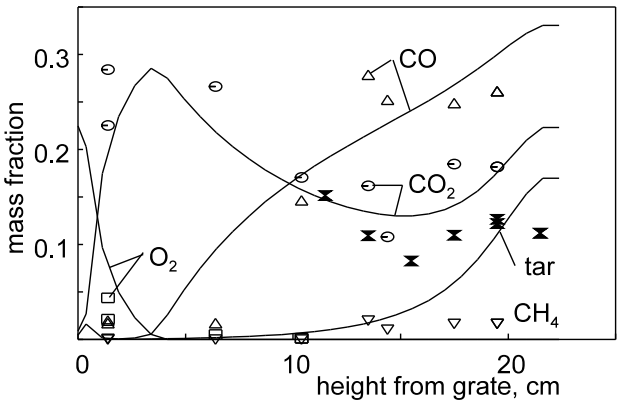

Fig. 4: Measured (points) and predicted (curves) concentrations of gas-phase species as a function of height from the grate. All quantities are presented as kg per kg of tar-free gas. Predictions are after 2 hours of operation.

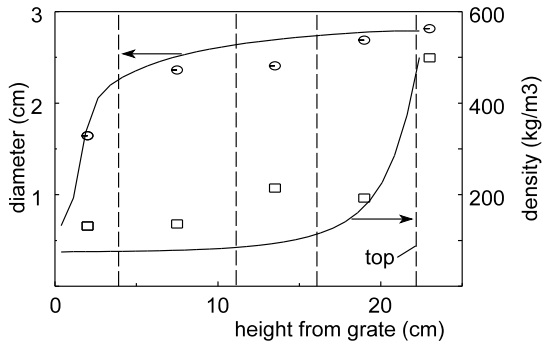

Fig. 5: Measured and predicted fuel particle size and density. Vertical lines indicate the boundaries of the sample slices for which the experimental points are averages. Predictions are for end of test (roughly 4 hours of operation).

Figs. 5 and 6 show the results of bed sampling, each point being an average over 6-8 particles. Pyrolysis causes a rapid decrease in particle density near the top of the bed, while the diameter does not change substantially until pyrolysis is finished. The good agreement between model and predictions substantiates the assumption that pyrolysis occurs at constant volume. Fig. 6 shows the ash buildup on the grate and the progress of pyrolysis as reflected in the ASTM volatiles content of the fuel. Owing to the low ash content of the fuel, changes in the structure of the bed caused by ash buildup were very small; there is, for example, little difference between the predicted gas phase profiles in Fig. 4 and those two hours later at the end of the experimental run. This contrasts with the large effects observed in earlier work with coke [2]. The temperature profiles in Fig. 7 show that gas temperatures near the bottom of the bed are much higher than solid temperatures, owing to gas phase oxidation of CO. Measured temperatures are close to predicted solid temperatures because of the intense radiation between neighbouring particles.

Conclusions

Despite the crudity of the pyrolysis model presented here, the numerical predictions give encouraging agreement with experimental data. The tar probe introduced here appears to be a practical means of sampling tar *in situ* in a burning wood bed.

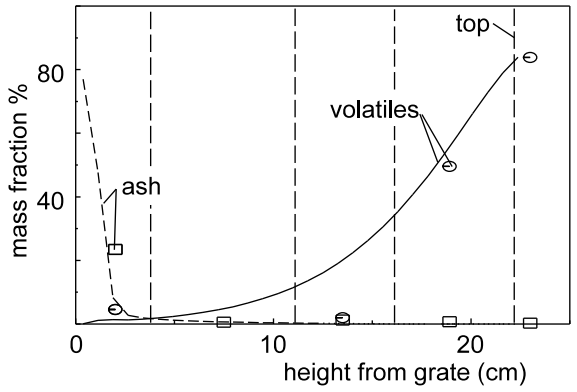

Fig. 6: Measured and predicted volatiles content and ash mass fractions in the bed as determined by ASTM D3172 proximate analysis. Predictions are for the end of the experiment (about 4 hours).

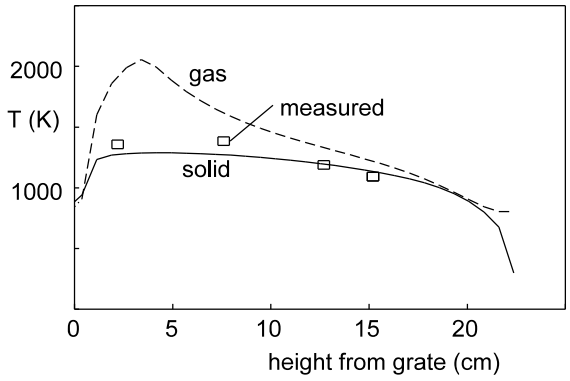

Fig. 7: Measured and predicted temperatures in the bed.

Acknowledgement

The authors are grateful to NSERC for funding this work.

Nomenclature

a_{BC}	fuel particle specific surface in bed, m^2/m^3	X_F	volume fraction of fuel in solids	**Subscripts**	
D	diffusivity, m^2/s	Y	mass fraction	C	char
G	net carbon flux, kg/m^2s	α	ash mass fraction in fuel	F	fuel
G_P	volatiles flux, kg/m^2s	ϵ	void fraction	i	individual species
k_Y	mass transfer coefficient, kg/m^2s	ζ_C	char yield, mass fraction of fuel	P	pyrolysis gas (volatiles)
r	reaction rate, kg/m^3 bed /s	ρ	density, kg/m^3	R	at surface of particle
v	superficial velocity, m/s	χ	mass fraction of species in pyrolysis products	S	solid phase (fuel + ash)
W	fractional conversion			T	tar
				W	unconverted fuel (“wood”)
				0	initial value

References

[1] Cooper, J., Hallett, W.L.H., *Chemical Eng. Science* **55**, 4451 (2000)
[2] Ryan, J.S., Hallett, W.L.H., *Chemical Eng. Science* **57**, 3873 (2002)
[3] Grønli, M.G., Varhegyi, G., Di Blasi, C., *Ind. Eng. Chem. Research* **41**, 4201 (2002).
[4] Órfão, J.J.M., Antunes, F.J.A., Figueiredo, J.L., *Fuel* **78**, 349 (1999).
[5] Antal, M.J., Varhegyi, G. *Ind. Eng. Chem. Research* **34**, 703 (1995).
[6] Koufopanos, C.A., Papayannakos, N., Maschio, G., Lucchesi, A., *Can. J. Chem. Eng.* **69**, 907 (1991).
[7] Grønli, M.G., Melaaen, M.C., *Energy and Fuels* **14**, 791 (2000).
[8] Larfeldt, J., Leckner, B., Melaan, M.C., *Biomass & Bioenergy* **18**, 507 (2000).
[9] Gupta, M., Yang, J., Roy, C., *Fuel* **82**, 919 (2003).
[10] Reid, R.C., Prausnitz, J.M., Poling, B.E., *The Properties of Gases and Liquids* (4th ed.), New York, McGraw-Hill.
[11] Ryan, J.S., Hallett, W.L.H., and Di Iorio, J., Combustion Inst. Canadian Sect. 1999 Meeting